BEFORE AND AFTER THE CAYO COCO CAUSEWAY, CUBA: A CRITICAL VIEW FROM SPACE

Eudel Cepero and Angelique Lawrence

The Cuban archipelago is made up of 4,195 islands, cays, and islets, grouped into four main sub-archipelagos: Los Canarreos, De Los Colorados, Jardines de la Reina, and Jardines del Rey. Until the late 1980s, Jardines del Rey, the largest of the Cuban sub-archipelagos with some 400 cays and islets, had mostly pristine landscapes of mangroves, matorral, and evergreen vegetation that provided habitat for nearly 1,250 species of wildlife, 20 percent of which were endemic to this Cuban sub-archipelago. Also deserving of special mention are the marine ecosystems of small inland coastal lakes and extended sand beaches of the Jardines del Rey, which are well protected by large coastal fossil sand dunes.[1]

In 1986, a long causeway was built over the shallow waters of Bahía de los Perros (Dogs Bay) on the northern part of the Cuban archipelago. This causeway is also known as "Pedraplen de Cayo Coco," as it connects the north coast of Cuba with Cayo Coco, the largest offshore cay in the Jardines del Rey sub-archipelago. The Cayo Coco causeway is 26 kilometers long, 8 meters wide, and 2.66 meters high over the mid ocean level. It was built over ocean depths up to 3 meters (Figure 1).[2]

Figure 1. View of the Cayo Coco Causeway

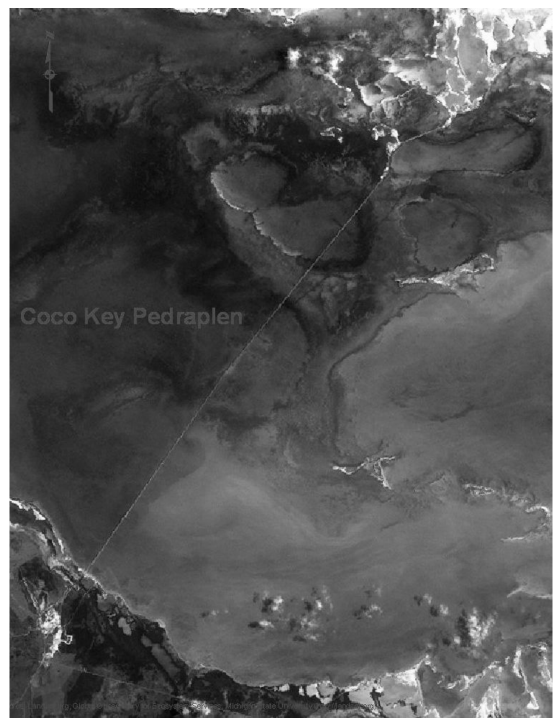

The Cayo Coco causeway raises several environmental concerns as it cuts Bahía de los Perros in half, with an inefficient design and distribution of bridges that do not consider the natural movement of currents inside the bay. To the west side of the causeway there is still interchange of currents with the open ocean but to the east side, very little occurs due its construc-

1. Eudel Cepero, "Dolor en los cayos," *Encuentro de la Cultura Cubana*, vol 21–22, verano-otoño 2001, pp. 93–94.

2. J. Torres. No date. *Diseño de carreteras en el mar: Los pedraplenes*. Empresa de Proyectos de Obras del Transporte, http://www.gecgr.co.cu/infoconst/bvirtual/cd/envios/envio%20610.pdf (downloaded 4/17/2006).

tion.[3] As a result, the movement of nutrients and phytoplankton, and the interchange of temperature and organic matter, have also changed, affecting the entire ecosystem. In addition, the causeway increases the content of silicates (2.35µmol/L) and ammonia (21.07µmol/L) in the water and decreases the dissolved oxygen content down to 81.8%. From a hydrochemistry point of view, the waters of Bahía de los Perros have been severely affected.[4] A dramatic increase in salinity has also been reported because of the causeway's construction.[5] Water samples taken from Bahía de los Perros in 2005, showed elevated salinity ranges between 50–80 ppm.[6]

The mangrove populations located in the primary coastal region to the south of Cayo Coco facing Bahía de los Perros is mostly Avicennia germinans (black mangrove), with canopies between 5–10 meters above sea level, and with a naturally high salinity tolerance.[7] A scientific ground report indicated high mortality of black mangrove to the southeast of Cayo Coco precisely due to the increase in salinity caused by the pedraplen.[8] There is also a local news report from 1997 indicating that 5,300 hectares (53 x 10^6 m^2) of mangrove have been destroyed around Bahía de los Perros.[9] Also associated with these environmental impacts are other phenomena such as drastic reduction of commercial fish stock in the area. According to local reports, 1990 was the lowest fishing year in the fishing Port of Punta Alegre, located a few miles to the west of the Cayo Coco causeway.[10]

Our hypothesis is that there has been an overall reduction in mangrove coverage within Bahia de los Perros between 1990 and 2000. It is believed that the construction of the pedraplen, which is hindering and changing the movement of the ocean currents and has resulted in a significant increase in water salinity within the bay, may be the cause of the destruction of these large mangrove populations. This paper is intended to make a comparative remote sensing evaluation of changes in mangrove coverage before and after the construction of the Cayo Coco causeway in Bahía de los Perros in order to potentially account for the reduced mangrove area.

METHOD

MultiMate satellite data has historically been used to investigate changes in the extent of mangrove coverage. Remote sensing data from satellite sensors such as Landsat has also been used to provide information regarding coverage extent, conditions, and boundaries of coastal wetlands. This suggests that mangrove biophysical variables can be measured directly via remote sensing.[11] In this case however, the intention is to assess the changes in mangrove population in the Bahía de los Perros before and after the causeway's

3. Colectivo del autores, "Interpretación digital de imágenes en la evaluación de impactos ambientales en el archipiélago Sabana-Camagüey, Cuba," *Revista Internacional de Ciencias de la Tierra*, July 2002, http://www.mappinginteractivo.com/plantilla-ante.asp?id_articulo=144 (downloaded 4/17/2006).

4. I. Rodríguez and I. García, *Hidro-química y calidad ambiental del archipiélago Sabana-Camagüey*, Proyecto GEF/PNUD CUB/92/631, 2002. http://puma.sskkii.gu.se/cubataller7/IVTaller/hidro6.html (downloaded 8/12/2005).

5. P. Alcolado, E. García, and N. Espinosa, *Una estrategia para la protección de la biodiversidad y el progreso hacia el desarrollo sustentable en el ecosistema Sabana-Camagüey (parte-II)*, Proyecto GEF/PNUD CUB/92/G31, 1999, http://www.mappinginteractivo.com/plantilla-ante.asp?id_articulo=116 (downloaded 3/10/2006).

6. L. Menéndez, J. Guzmán, R.Capote, A. González and L. Rodríguez, "Variabilidad de los bosques de manglares del archipiélago Sabana-Camagüey: Implicaciones para su gestión," *Revista Internacional de Ciencias de la Tierra*, Marzo 2005, http://www.mappinginteractivo.com/plantilla-ante.asp?id_articulo=874 (downloaded 3/13/2006).

7. Ibid.

8. Alcolado et al., ob. cit.

9. Ortelio González Martínez, "El naufragio de las especies," Newspaper *Invasor*, January 11, 1997.

10. Ibid.

11. Y. Hussin, M. Zuhair, and M. Weir, "Monitoring Mangrove Forests using Remote Sensing and GIS," International Institute for Aerospace Survey and Earth Science (ITC), 1999. http://www.gisdevelopment.net/aars/acrs/1999/ps5/ps5126.asp (downloaded 3/31/2006).

construction, rather than conduct any biological or species evaluation of the mangroves. The primary goal of this project therefore, is the measurement of changes in the mangrove population over time, particularly since the causeway was built.

There are several vegetative indices that allow radiometric measurements to determine relative abundance and activity of green vegetation from one growing season to the next, from year to year, or from decade to decade. For the purpose of this project, the Normalized Difference Vegetative Index (NDVI) was used. The NDVI is calculated as the ratio between measured reflectivity in the red and near infrared (NIR) portions of the electromagnetic spectrum. These two spectral bands are chosen because they are most affected by the absorption of chlorophyll in leafy green vegetation and by the density of green vegetation on the surface. Higher NDVI values are associated with higher levels of healthy vegetation cover, while lower values indicate stressed or unhealthy vegetation. NDVI values can range from -1.0 to 1.0, but vegetation values typically range between 0.1 and 0.7.[12] There are several formulas to calculate NDVI, however for this study we used the following one:[13]

$$NDVI = (NIR - red) / (NIR + red)$$

The spectral resolution for mangrove assessment usually involves the green, red, and infrared bands of remotely sensed satellite data, used to derive false color composites on spatial resolutions of 30 and 60 meters. For this study two orthorectified Landsat images of north-central Cuba were used for two epochs: 1990 TM, and 2000 ETM+. The descriptions of the 1990 and 2000 datasets are given at Appendix 1 and 2, respectively.

Since erroneous NDVI estimates can result in mistakes calculating mangrove loss, a radiometric correction was made to improve the accuracy of surface spectral reflectance on the two images (1990 and 2000) by using the ERDAS IMAGINE graphical user interface.[14] The radiometric correction was initiated by first running a "bandstacker" model, which stacks together all the spectral bands except the thermal infrared band. Following this, conversion of Digital Numbers (DN) to absolute radiance values was made by also using two ERDAS models, one for each image. This is necessary as each sensor has its own calibration parameters used in recording the DN values, and the same DN values in each of the images taken by two different sensors may represent two different radiance values. A conversion from radiance to sensor reflectance was then made by using another model that was applied to both images. The primary purpose of converting spectral radiance to at-sensor reflectance is to standardize the effect of illumination geometry, thus helping to reduce between-scene variability. Figure 2 shows the two images generated following the series of model conversions and corrections. Note that the causeway is visible in the 2000 image.

A "striping" effect was observed in the corrected 1990 image, which became more apparent after the ERDAS NDVI tool was applied to each of the output reflectance images (Figure 3). It was therefore necessary to conduct a Fast Fourier transformation to the 1990 Band 4 NIR, the band in which this "striping" was observed. This detects and corrects spatial repetitive patterns and converts the output to a Fourier image file, but the resultant image still remained with the "striping" within the central water regions. A "de-striping tool" in ERDAS was then applied instead, but this left a "smearing" effect (Figure 4). Finally a model was applied that subtracts all water pixels (where the NDVI was less than or equal to zero and where the image irregularities were occurring) to finally fix the problem (Figure 5).

12. RangeView website. The University of Arizona. *Normalized Difference Vegetation Index (NDVI).* http://rangeview.arizona.edu/glossary/ndvi.html (4/19/2006).

13. John R. Jensen, *Introductory Digital Image Processing: A Remote Sensing Perspective*, Third Edition (Upper Saddle River, New Jersey: Prentice Hall Series in Geographic Information Science, 2005), p. 311.

14. ERDAS Imagine. Leica Geosystems. http://www.gis.leica-geosystems.com/LGISub1x33x0.aspx (downloaded 4/19/2006).

Figure 2. Corrected Satellite Images of Bahía de los Perros, 1990 (top) and 2000 (bottom)

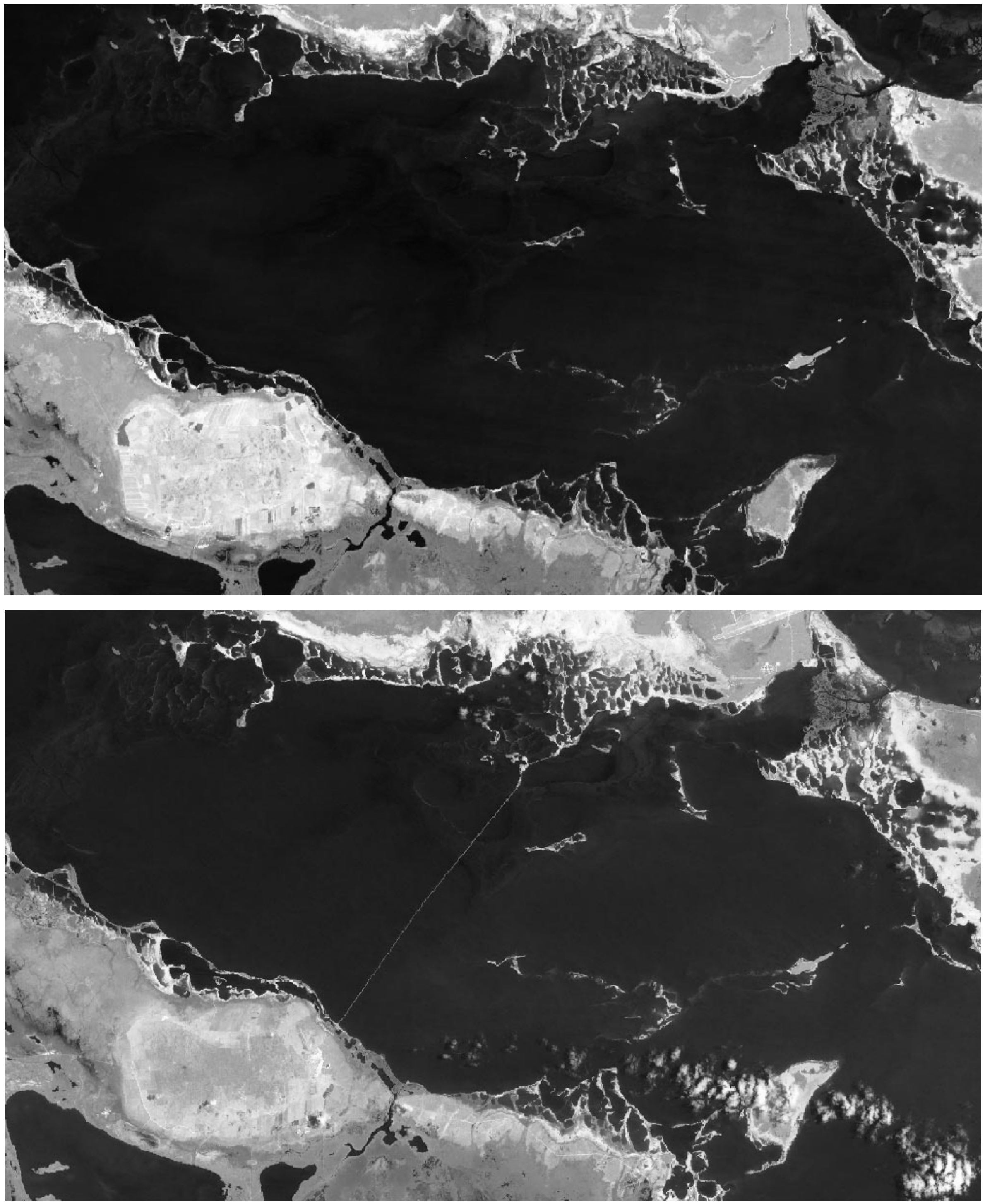

A model calculating the difference between the 2000 and 1990 NDVI outputs was applied to get a differentiated NDVI output image showing the decrease in vegetation from 1990 to 2000. The values ranged between -0.25 and -0.1, which represents loss of vegetation and therefore some degree of mangrove damage. Based on this range, the output raster was then reclassified into four NDVI classes: the extreme neg-

Figure 3. "Striping" Effect on the 1990 NDVI Satellite Image

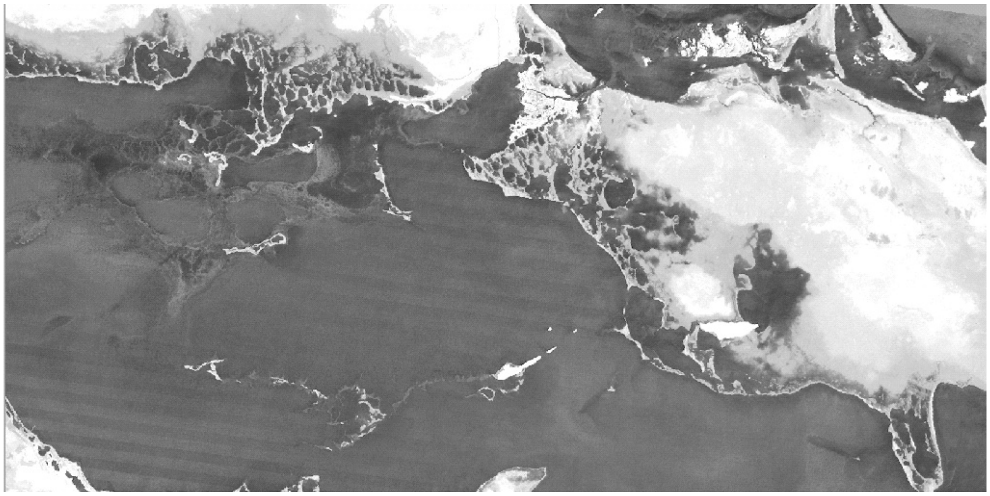

Figure 4. "Smearing" Effect on 1990 Satellite Image following Fast Fourier

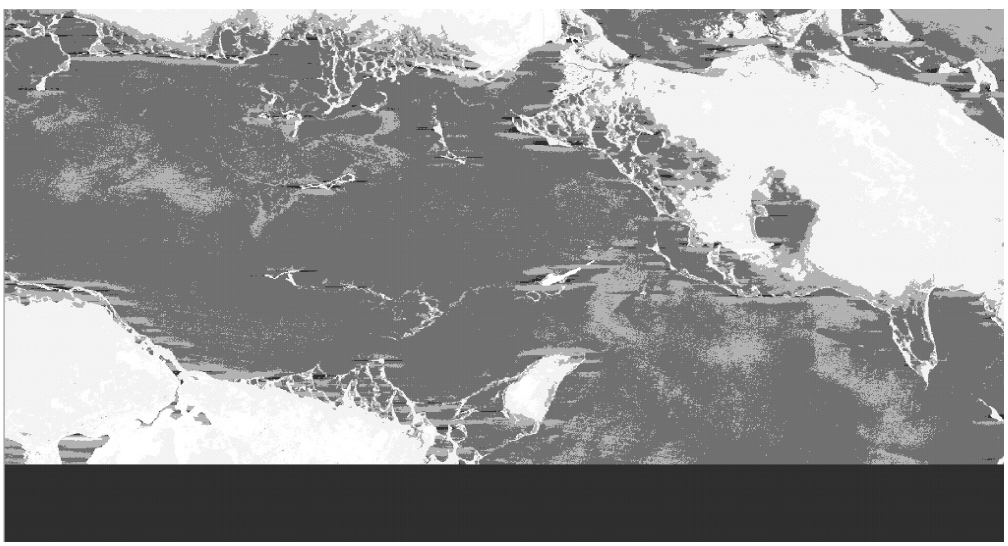

ative values (-0.25) representing areas of most significant mangrove damage and the values closer to 0 indicating areas of lesser or insignificant mangrove damage. A GIS vector shapefile of the Cuban mangrove land cover was then converted to a raster image and used as a mask to extract NDVI values representative of mangrove cover only (Table 1). Finally, the output image was imported into a GIS for display (Figure 6). It was then possible to calculate the area of mangrove loss from the pixel values displayed for each class of the raster attributes.

DISCUSSION

As previously mentioned, higher NDVI values are associated with higher levels of healthy vegetation cover, and lower values with stressed or unhealthy vegetation. The output image of the model subtracting 2000 NDVI from 1990 NDVI shows in different colors the areas of significant mangrove destruction, stressed/unhealthy mangrove populations, and minor mangrove damage. There are 6,505,200 m^2 of mangrove vegetation that was almost completely destroyed. It is interesting to note that our results corre-

Figure 5. Final Output 1990 NDVI with All Stripes and Smears Erased

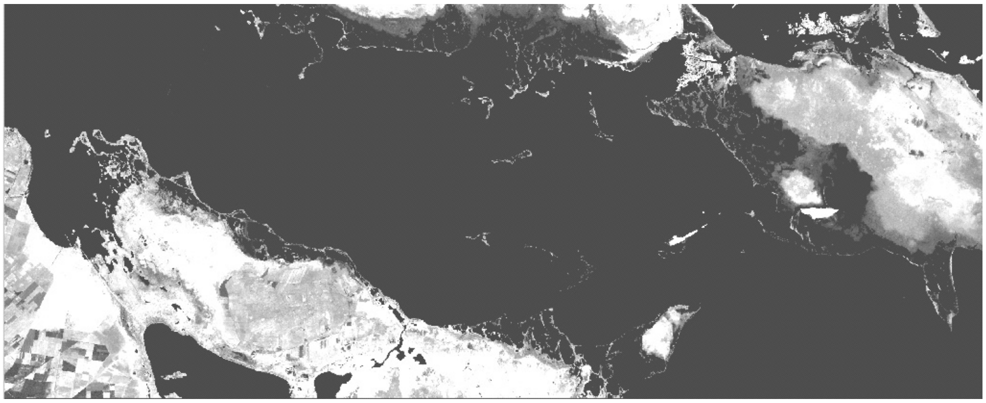

Table 1. Relative Health of Mangrove

NDVI Classes	NDVI Class Ranges	Pixels (30x30)m²	Area (M²)	Color	Description
0	-0.1	462,259	416,033,100	-	No Significant Mangrove Damage
1	-0.15 -0.1	18,315	16,483,500		Minor Mangrove Damage
2	-0.25 -0.15	16,265	14,638,500		Stressed/Unhealthy Mangrove Populations
3	-0.25	7228	6,505,200		Significant Mangrove Destruction

Figure 6. NDVI Values for Bahia de los Perros Study Area, Cuba

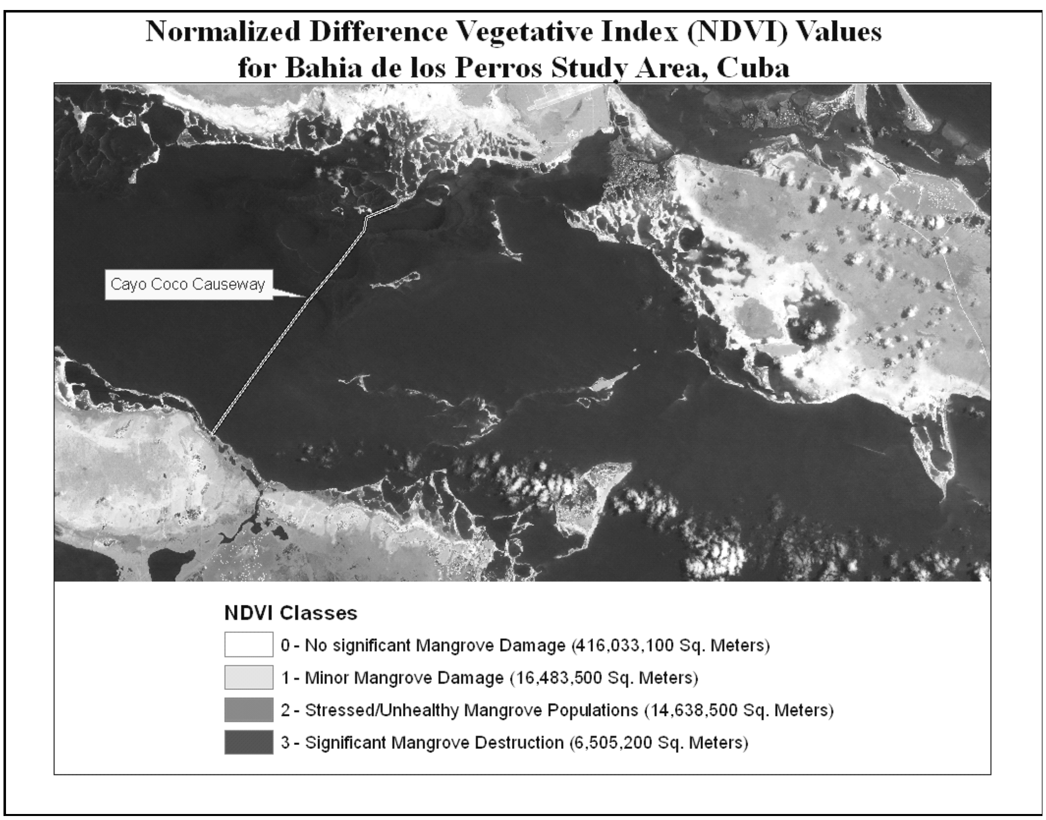

Figure 7. Small Mangrove Island Severely Affected by the Construction of the Cayo Coco Causeway

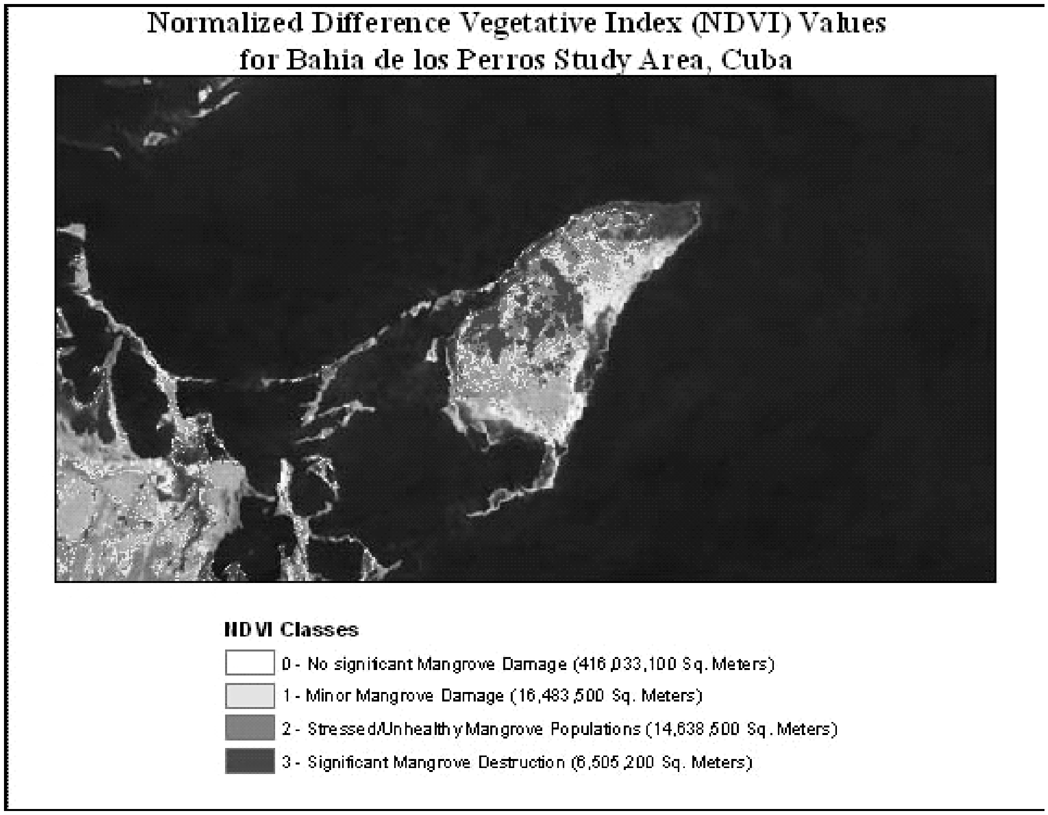

late with a previously-cited scientific ground report which indicated high mortality of black mangrove to the southeast of Cayo Coco (depicted by the darker areas in Figure 6). In addition, it is the east side of the causeway where the darker—or more environmentally affected—areas are the most coincident with the higher levels of water salinity. In this area there are several small mangrove islands which were severely affected, one of which can be see in Figure 7. Also, to the south, where the causeway is connected to Cayo Coco, there are several chains of mangrove islands that were also severely affected.

A total of 37,627,200 m^2 of mangrove was affected in some way by the construction of the causeway. This represents 70% of the area reported by a local news paper in 1997 for the entire Bahía de Los Perros. This difference in percentage, however, is likely due to the fact that only a portion of this area was analyzed during our study. Considering that this evaluation is covering a period of 10 years (from 1990 to 2000) with significant mangrove damage, it can be assumed that the situation is worse today if the causes of the mangrove loss still persist. It may be useful therefore, to determine the current situation by conducting this same type of analysis using more recent satellite imagery.

This type of historical NDVI calculation can be applied to account for loss of mangrove or any other type of vegetation once the appropriate satellite imagery is available to perform a historical environmental impact assessment of other causeways built in a similar manner.

CONCLUSION

The NDVI analysis indicates that there was less mangrove coverage in the Bahía de los Perros in 2000 than in 1990, which is likely to have resulted from the construction of the Cayo Coco causeway. The causeway altered the movement of ocean currents, increased the salinity, and ultimately impacted the mangrove ecosystem. Based on this evaluation, it is strongly recommended that steps be taken to restore the natural movement of water within Bahía de los Perros to the patterns present prior to the construction of the Cayo Coco causeway.

APPENDIX 1
LANDSAT THEMATIC MAPPER DATA (1990s)[15]

Output Product Specifications:

- Spectral Bands: All seven Landsat TM bands - 3 visible, 1 NIR, 2 SWIR, and 1 thermal IR
- Coverage: Single Landsat WRS Path/Row
- Projection/Datum: UTM / WGS84
- Pixel size: 28.5 meters
- Interpolation Method: Nearest Neighbor
- Absolute Positional Accuracy: 50 meters RMS.

Source (Input) Data:
Imagery:

- Spectral Bands: All seven Landsat TM bands
- Coverage: Single Landsat WRS Path/Row
- Projection/Datum: SOM / WGS84
- Pixel Size: Mixture of 28.5 and 30 meters
- Interpolation Method: Cubic Convolution
- Orientation: Path oriented
- Coverage Date: Scene dependent (nominally 1990 +/- 3 years).

Control:

- Horizontal: Controlled scenes contained 6 to 12 photo-identifiable points with absolute positional accuracy not greater then 15.0 meters RMS.
- Vertical: DTM with 3–arc second postings where available. Where 3–arc second data not available, GTOPO30 (30–arc second) digital elevation models are used.

Digital Image Processing:

- Photogrammetric Block Adjustment:
  Performed using Earth Satellite Corporation's proprietary photogrammetric software
- Orthorectification:
  Resampled to a UTM/WGS84 projection using nearest neighbor (i.e. no interpolation).Image Enhancements:
  The data are spatially and spectrally unenhanced

APPENDIX 2
LANDSAT ENHANCED THEMATIC MAPPER PLUS DATA (2000s)[16]

Output Product Specifications:

- Spectral Bands: All nine Landsat ETM+ bands - 3 visible, 1 NIR, 2 SWIR, 1 Panchromatic, and 2 thermal IR
- Coverage: Single Landsat WRS Path/Row
- Projection/Datum: UTM / WGS84
- Pixel size: 14.25, 28.5, and 57 meters
- Interpolation Method: Nearest Neighbor
- Absolute Positional Accuracy: 50 meters RMS.

Source (Input) Data:
Imagery:

- Spectral Bands: All nine Landsat TM bands
- Coverage: Single Landsat WRS Path/Row
- Projection/Datum: SOM / WGS84
- Pixel Size: Mixture of 28.5 and 30 meters
- Interpolation Method: Cubic Convolution
- Orientation: Path oriented
- Coverage Date: Scene dependent (nominally 2000 +/- 1 years)

Control:

- Horizontal: Controlled scenes contained 6 to 12 photo-identifiable points with absolute positional accuracy not greater then 15.0 meters RMS.
- Vertical: DTM with 3–arc second postings where available. Where 3–arc second data not available, GTOPO30 (30–arc second) digital elevation models are used

Digital Image Processing:

- Photogrammetric Block Adjustment:
  Performed using Earth Satellite Corporation's proprietary photogrammetric software.
- Orthorectification:
  Resampled to a UTM/WGS84 projection using nearest neighbor (i.e. no interpolation)
- Image Enhancements:
  The data are spatially and spectrally unenhanced

15. http://www.landsat.org/dataservices/Landsat_ortho/Dataset_Description.htm (downloaded 4/19/2006).
16. http://www.landsat.org/dataservices/Landsat_ortho/Dataset_Description.htm (downloaded 4/19/2006).